Proceedings of the American Control Conference
Arlington, VA June 25-27, 2001

LARGE ENVELOPE FLIGHT CONTROL SATISFYING H_∞ ROBUSTNESS AND PERFORMANCE SPECIFICATIONS

Paul Blue[1,*], Levent Güvenç[2,#] and Dirk Odenthal[*]

[*]*Robust Control Group, Institute of Robotics and Mechatronics*
German Aerospace Center (DLR) - Oberpfaffenhofen
Postbox 1116, D-82230, Wessling, Germany
Fax.: +49-8153-28-1847, e-mail: blue@aem.umn.edu

[#]*Department of Mechanical Engineering, İstanbul Technical University*
Gümüşsuyu, Taksim, İstanbul TR-80191, Turkey

Abstract: A method of designing large envelope flight controllers for high performance aircraft is presented. The approach combines the simple two-degree of freedom architecture often referred to as a disturbance observer and recent advances in parameter-space control design techniques to form a new approach for large envelope flight control design. The procedure enables the designer to explicitly define the desired closed-loop dynamics and ensures that the closed-loop is stable and satisfies weighted frequency response magnitude (H_∞) specifications. The result is a straightforward procedure that enables the design of a robust flight controller that "forces" the closed-loop dynamics to behave like the specified 'desired dynamics' despite disturbances, modeling uncertainties, and variations in aircraft dynamics due to changing flight conditions. The procedure is presented by designing a pitch-rate controller for the F-16 Variable Stability In-Flight Simulator Test Aircraft (VISTA). The controller provides predicted 'Level 1' flying qualities throughout the large design flight envelope, which is demonstrated using both linear simulations and a high fidelity, nonlinear simulation. Finally, the controller is compared to a 7^{th} order and a 10^{th} order linear parameter-varying (i.e. gain-scheduled) controller and found to provide better performance and robustness.

1. INTRODUCTION

The design of flight control systems for fighter aircraft is an extremely demanding task. These aircraft must meet stringent performance specifications (MIL-STD-1797A, 1990) throughout a large envelope of operating conditions despite large variations in system dynamics (including variations in open-loop stability), which result from varying operating conditions and the presence of significant nonlinearities. Due to these large variations in the dynamics of the aircraft, it is often impossible to achieve the required level of performance throughout the flight envelope with a fixed controller. Practically, this results in the design of several controllers at trim points throughout the flight envelope, which are then scheduled with operating condition. While this gain-scheduling procedure has been successfully implemented on a number of fighter aircraft, it is extremely tedious and time consuming. The complex task of traditional gain-scheduling has resulted in a significant amount of research in recent years to develop methods of designing linear parameter-varying (LPV) controllers, which are "automatically" gain-scheduled (e.g. Blue & Banda, 1997).

In this paper, a much simpler approach for designing large envelope flight controllers is presented that provides the desired performance throughout the design envelope without gain-scheduling. The procedure combines the two-degree of freedom control architecture often referred to as a disturbance observer (Ohnishi, 1987; Umeno & Hori, 1991) and recent advances in parameter-space control design techniques (Odenthal & Blue, 2000) to form a new approach for designing flight controllers for high performance aircraft. The disturbance observer architecture is extremely attractive for a number of reasons, most notably, its insensitivity to disturbances and model uncertainty and its unambiguous structure, which enables the explicit definition of the desired closed-loop dynamics. The parameter-space technique of Odenthal & Blue, (2000) extends traditional parameter-space techniques (Ackermann et al., 1993) to enable the mapping of frequency response specifications into parameter-space; consequently, providing a straightforward and transparent way of selecting parameters in a fixed control structure (e.g. disturbance observer) to satisfy H_∞ robustness and performance specifications. The proposed design procedure is presented by designing a pitch rate controller for the F-16 Variable Stability In-Flight Simulator Test Aircraft (VISTA) that provides Level 1 flying qualities over a large flight envelope. The design example not only demonstrates the simplistic power of the proposed procedure, but also results in a controller that provides better results (without

[1] participant in the U.S. Air Force's Engineer and Scientist Exchange Program
[2] acknowledges support of the Alexander von Humboldt Foundation

gain-scheduling and without angle-of-attack feedback) than previous LPV control designs.

The remainder of the paper is organized in four main sections. An LPV model of the F-16 VISTA and the specifications used in the design example are reviewed in Section 2. The proposed large envelope flight control design approach is presented in Section 3 by designing a robust pitch-rate controller for the F-16 VISTA. Linear and nonlinear simulations are used in Section 4 to illustrate the effectiveness of the proposed approach, and the results are compared with previous LPV control results. The final section provides a summary.

2. F-16 VISTA: PITCH-RATE CONTROL

VISTA is a modified F-16 with the capability of simulating advanced aircraft configurations and testing advanced flight control concepts. In this section, an LPV model of the F-16 VISTA's short-period dynamics and design specifications for an F-16 pitch-rate controller are reviewed. The same model and objectives were used in (Spillman et al., 1996; Blue & Banda, 1997) and are being used here to demonstrate the advantages of the procedure presented and to facilitate the comparison of the results. For a detailed description of the model see (Spillman et al., 1996).

2.1 LPV Model

The actual longitudinal dynamics of the VISTA aircraft, which vary significantly with flight condition (i.e. altitude h and Mach number M), are denoted by $\mathcal{P}(h,M)$. For the pitch-rate control design, $\mathcal{P}(h,M)$ is modeled using the standard short period equations of motion (1) and a first order approximation of the actuator dynamics (2).

$$\frac{d}{dt}\begin{bmatrix}\alpha\\ q\end{bmatrix}=\begin{bmatrix}Z_\alpha & 1\\ M_\alpha & M_q\end{bmatrix}\begin{bmatrix}\alpha\\ q\end{bmatrix}+\begin{bmatrix}Z_{\delta_e}\\ M_{\delta_e}\end{bmatrix}\delta_{ed} \qquad (1)$$

where, α is the angle-of-attack, q is the pitch-rate, and δ_{ed} is the elevator deflection.

$$\delta_{ed} = P_{act}\delta_{ec}$$
$$P_{act} = \frac{-20.2}{s+20.2} \qquad (2)$$

where, δ_{ec} is the elevator command. Note that the negative sign in (2) is simply a result of the sign convention used.

At trimmed level flight, the dimensional coefficients Z_α, M_α, M_q, Z_{δ_e} and M_{δ_e} depend mainly on the altitude and Mach number. An LPV version of (1) for VISTA was developed by trimming and linearizing the Air Force Research Laboratory's high fidelity nonlinear simulation model of the F-16 VISTA at the operating conditions

M=[0.35 0.45 0.55 0.65 0.75 0.85]
h=[1,000 5,000 15,000 25,000] (ft)

and fitting the corresponding data for the dimensional coefficients with polynomial functions of M and h. The resulting expressions for the coefficients are:

$$\begin{aligned}
Z_\alpha &= 0.22 - 4.1\cdot 10^{-7}h - 2.6M + 5.15\cdot 10^{-5}Mh\\
M_\alpha &= 17.1 - 8.07\cdot 10^{-4}h - 68.4M\\
&\quad + 3.31\cdot 10^{-3}Mh + 56.2M^2 - 2.92\cdot 10^{-3}M^2h\\
M_q &= -0.228 + 7.06\cdot 10^{-6}h - 2.12M\\
&\quad + 4.86\cdot 10^{-5}Mh\\
Z_{\delta_e} &= -1.38\cdot 10^{-3} + 8.75\cdot 10^{-8}h - 0.34M\\
&\quad + 7.98\cdot 10^{-6}Mh\\
M_{\delta_e} &= -8.16 + 1.73\cdot 10^{-4}h + 40.6M\\
&\quad - 8.96\cdot 10^{-4}Mh - 99.3M^2 + 2.42\cdot 10^{-3}M^2h
\end{aligned} \qquad (3)$$

The LPV model obtained when these polynomial expressions (3) are used with (1) is denoted by $P_{LPV}(h,M)$. Then, the model used to represent $\mathcal{P}(h,M)$ for the pitch-rate control design is given by

$$P(h,M) = P_{LPV}(h,M)\cdot P_{act} \qquad (4)$$

and accurately represents the F-16 VISTA's short period dynamics throughout the flight envelope $h\in$[5,000ft 25,000ft] and $M\in$[0.4 0.8]. Of course, even though $P(h,M)$ accurately represents $\mathcal{P}(h,M)$, there are obviously modeling errors, which results in model uncertainty denoted by Δ_m, where Δ_m represents the difference (in a multiplicative sense) between the actual aircraft dynamics and the model (4). That is,

$$\mathcal{P}(h,M) = P(h,M)\cdot(1+\Delta_m) \qquad (5)$$

2.2 Pitch-Rate Control Design Specifications

The design objective here and in (Spillman et al., 1996; Blue & Banda, 1997) is to design a controller for the F-16 VISTA that provides robust pitch-rate command tracking with predicted Level 1 handling qualities throughout the design envelope $h\in$[5,000ft 25,000ft] and $M\in$[0.4 0.8]. Time domain handling quality specifications for the pitch-rate response (MIL-STD-1797A, 1990) are shown in Figure 1 and Table 1.

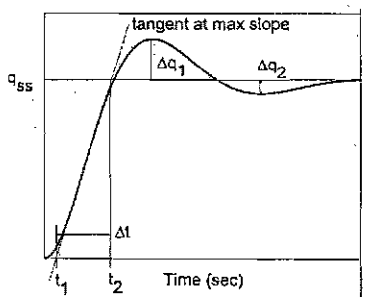

Figure 1. Piteh-rate handling qualities specifications

Table 1: Pitch-Rate Handling Qualities Specifications		
Parameter	Level I	Level II
t_1 max	0.12 sec	0.17 sec
$\Delta q2/\Delta q1$	0.30	0.60
Δ_t max	$500/V_T$ sec	$1600/V_T$ sec
Δ_t min	$9/V_T$ sec	$3.2/V_T$ sec
V_T represents the true velocity {ft/sec}		

With these handling qualities specifications in mind, a reference model that provides a Level 1 pitch-rate response over the entire design envelope was selected in Spillman et al., (1996) and is given by,

$$P_d = \frac{4^2}{s^2 + 2 \cdot 0.5 \cdot 4 \cdot s + 4^2} \tag{6}$$

In the sequel, the reference model P_d will be referred to as the "desired dynamics". Spillman et al. (1996) and Blue & Banda, (1997) used P_d (6) and $P(h,M)$ (4) in a weighted model matching design structure (with uncertainty and disturbances) to design LPV controllers that provided a closed-loop response that matches the response of P_d throughout the design envelope. A version of this weighted model matching design structure is used in Section 3.2 to design a pitch-rate controller using the design procedure proposed in this paper.

3. LARGE ENVELOPE FLIGHT CONTROL DESIGN

In this section, a new approach for designing large envelope flight controllers for high performance aircraft is demonstrated by designing a pitch-rate controller for the F-16 VISTA aircraft. First, the control architecture is presented, and then parameter-space design techniques are used to obtain a controller that satisfies the design specifications presented in Section 2.2.

3.1 Control Architecture and Design Objectives

The control architecture proposed for large envelope flight control in this paper is based on a disturbance observer, which provides insensitivity to disturbances and model uncertainty. This control structure has been used successfully in a number of motion control applications (Ohnishi, 1987; Umeno & Hori, 1991; Güvenç and Srinivasan, 1994; Bünte et al., 2001; Aksun-Güvenç et al., 2001). The control architecture proposed for the VISTA pitch-rate controller is shown in Figure 2,

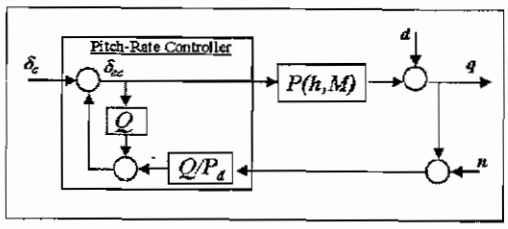

Figure 2. Pitch-rate controller architecture

where $P(h,M)$ denotes the open-loop aircraft dynamics from elevator command to pitch-rate response and P_d denotes the desired pitch dynamics of the aircraft. The two filters P_d and Q form the pitch-rate controller when utilized as shown in Figure 2. In general, designing the two degree of freedom controller shown in Figure 2 would involve the design of both the filter Q and the desired dynamics P_d. However, as in this example, P_d is usually selected independent of Q. Then, the objective is to design the filter Q so that a given pitch-rate command δ_c provides the desired response despite changing flight condition h-M, disturbanees d, sensor noise n, and model uncertainty. That is, design a Q so that the closed-loop represented by Figure 2 has

$$q = P_d \delta_c \tag{7}$$

as its input – output relation throughout the flight envelope. The relative degree of the filter Q is chosen to be at least equal to the relative degree of P_d for causality of Q/P_d.

Investigating the input-output transfer functions associated with the purposed architecture provides insight regarding the required form of Q and the expected characteristics of the resulting closed-loop. The loop-gain for the closed-loop aircraft represented by Figure 2 is

$$L(h,M) = \frac{P(h,M) \cdot Q}{P_d \cdot (1 - Q)} \tag{8}$$

The model regulation H, disturbance rejection (sensitivity) S, sensor noise rejection (complementary sensitivity) T, and performance H_p, transfer functions of the controlled system are given by

$$H(h,M) \equiv \frac{q}{\delta_c} = \frac{P_d \cdot P(h,M)}{P_d \cdot (1-Q) + P(h,M) \cdot Q} \tag{9}$$

$$S(h,M) \equiv \frac{q}{d} = \frac{1}{1 + L(h,M)} = \frac{P_d \cdot (1-Q)}{P_d \cdot (1-Q) + P(h,M) \cdot Q} \tag{10}$$

$$T(h,M) \equiv \frac{-q}{n} = \frac{L(h,M)}{1 + L(h,M)} = \frac{P(h,M) \cdot Q}{P_d \cdot (1-Q) + P(h,M) \cdot Q} \tag{11}$$

$$H_p(h,M) \equiv P_d - H(h,M) \tag{12}$$

It is obvious from (9) – (11) that Q must be a low pass filter with unity gain, which results in $q/\delta_c \to P_d$ and $q/d \to 0$ at low frequencies where $Q \to 1$ and $q/n \to 0$ at high frequencies where $Q \to 0$. In order to explicitly show the characteristics of this control architecture, Q is set to 1 in (9) and (10) to obtain

$$H_{Q=1}(h,M) = \frac{P_d \cdot P(h,M)}{P(h,M)} = P_d \tag{13}$$

$$S_{Q=1}(h,M) = \frac{0}{P(h,M)} = 0 \tag{14}$$

which clearly shows that good model regulation and disturbance rejection are achieved within the bandwidth of Q, (despite variations in $P(h,M)$). Of course, it is not possible to achieve model regulation or disturbance rejection at frequencies above the actuator's bandwidth, so nothing is gained by having the bandwidth of the Q filter significantly larger than that of the actuator. Furthermore, as shown by (11), limiting the bandwidth of Q is required to reject high frequency sensor noise. The design requirements specified in terms of the filter Q are summarized in Figure 3.

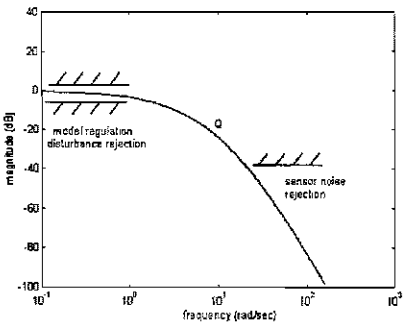

Figure 3. Q design requirements

3.2. Parameter-Space Control Design

In this seetion, parameter-space techniques (Ackermann et al., 1993; Odenthal & Blue, 2000) are used to design the filter Q to obtain a pitch-rate controller that satisfies the design objectives presented in Section 2.2. This is accomplished by mapping design specifications into the free paramcter space of Q. The desired dynamics given by (6) mandates a Q filter with a relative degree of at least two for implementation purposes (causality of Q/P_d). Opting for a simple controller, the Q filter structure is chosen as

$$Q = \frac{\omega_Q^2}{s^2 + 2\zeta_Q\omega_Q s + \omega_Q^2} \tag{15}$$

giving free parameters ω_Q and ζ_Q . Then, parameter-space methods are used to map the design requirements given by equations (16), (17), and (18) below, into the ω_Q-ζ_Q parameter plane resulting in the feasible region of the ω_Q-ζ_Q space (i.e. the set of ω_Q-ζ_Q that satisfy the mapping equations).

$$roots\{p_{ce}(h,M,\omega_Q,\zeta_Q)\} \subset \mathbb{C}^- \quad \text{(Hurwitz Stability)} \tag{16}$$

$$\left\| W_u \cdot T(h,M,\omega_Q,\zeta_Q) \right\|_\infty \le 1 \quad \text{(Robust Stability)} \tag{17}$$

$$\left\| W_p \cdot H_p(h,M,\omega_Q,\zeta_Q) \right\|_\infty \le 1 \quad \text{(Nominal Performance)} \tag{18}$$

Equation (16) ensures that all of the roots of the closed-loop characteristic equation given by

$$p_{ce}(h,M,\omega_Q,\zeta_Q) \equiv Numerator\{1 + L(h,M,\omega_Q,\zeta_Q)\} \tag{19}$$

are in the negative complex plane (i.e. ensures stability of the nominal closed-loop throughout the design envelope). In equations (17) and (18), T and H_p come from (11) and (12) and the weights W_u and W_p were taken from Spillman et al., (1996). The uncertainty weight W_u, is used to account for model uncertainties Δ_m (5), most notably unmodeled dynamics at high frequencies. Satisfying equations (16) and (17) ensures robust stability throughout the design envelope despite the uncertainties represented by W_u. The performance weight W_p penalizes the error between the desired and aetual pitch-rate; thus, satisfying (18) ensures that the actual response matchs the desired response to the accuracy specified by W_p. The interpretation of (17) and (18) can also be seen in Figure 4, where

$$\frac{e_u}{d_u} = W_u \cdot T(h,M,\omega_Q,\zeta_Q) \tag{20}$$

$$\frac{e_p}{\delta_c} = W_p \cdot H_p(h,M,\omega_Q,\zeta_Q) \tag{21}$$

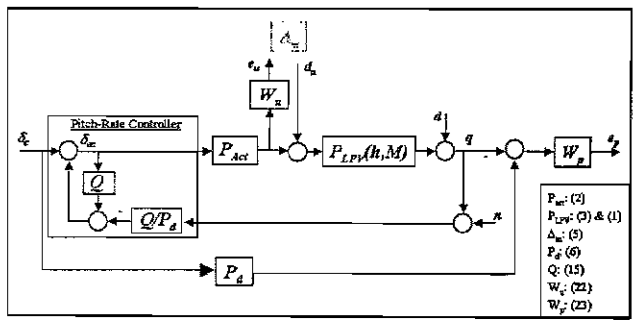

Figure 4. Weighted design model

After (16) – (18) are mapped to ω_Q-ζ_Q , the feasible region that simultaneously satisfies all three requirements is formed by the intersection of the feasible region obtained from each individual requirement. Note that sinee (16) – (18) depend on flight condition h-M , the set of feasible ω_Q-ζ_Q satisfying these equations also depends on h-M. Figure 5 shows the results of mapping (16) – (18) into ω_Q-ζ_Q for h=5000 ft and M=0.8.

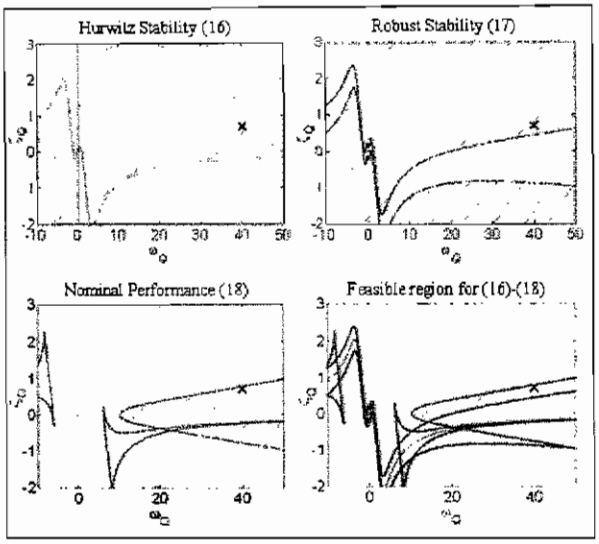

Figure 5. Feasible ω_Q-ζ_Q region for h = 5000 ft, M = 0.8

Since the objective is to design a controller that satisfies these specifications over the entire design envelope, (16) – (18) are mapped for as many additional operating conditions deemed necessary to ensure that the specifications are met throughout the design envelope. The region in the ω_Q-ζ_Q plane that satisfies (16) – (18) at the four "corners" of the design envelope is shown as the hatched regions in Figure 6. Note that for this design, the feasible region obtained by mapping the corners of the design envelope is not reduced by mapping additional flight conditions. The design is completed by picking one point from this feasible region. This can be done arbitrarily; however, if after mapping all design requirements, the feasible region is still large, additional demands can be placed on the controlled system. For example, the feasible solution that minimizes the structured singular value could be selected, or the original design specifications could be "tightened", as was done here. In this design, after mapping (16) – (18) using the original weights given in Spillman et al., (1996), the feasible region was so large, that the design was redone using a significantly more demanding uncertainty weight W_u. The final weights used to produce Figures 5 and 6 are given by

$$W_u = 2\frac{s + 0.2 \cdot 1256}{s + 2 \cdot 1256} \tag{22}$$

$$W_p = 0.4\frac{s + 100}{s + 4} \tag{23}$$

This W_u accounts for 200 times more uncertainty at low frequencies and 20 times more uncertainty at high frequeneies than the original weight used in Spillman et al., (1996) and Blue & Banda, (1997). After changing the uncertainty weight, the final design, which is marked with an **x** in Figures 5 and 6 was chosen (rather arbitrarily) as ζ_Q=0.7 and ω_Q=40 rad/s.

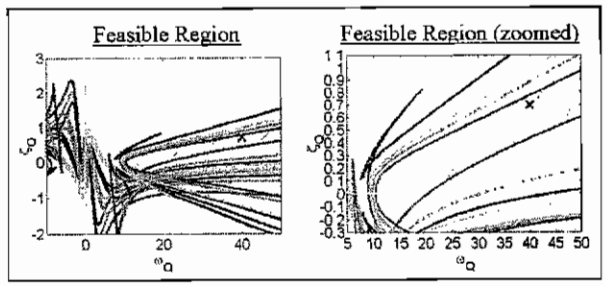

Figure 6. Feasible region obtained by mapping (16)-(18) into ω_Q-ζ_Q at the four corners of the design envelope

4. CONTROLLER EVALUATION

4.1 Simulations Results

Linear simulation were preformed throughout the design envelope using the controller designed in the previous section. The results corresponding to the four corners of the design envelope are shown in Figure 7, which also shows the pitch-rate command and the response of P_d (6). It is clear from this figure that the pitch-rate response demonstrates predicted Level 1 handling qualities for all four extremal flight conditions. As might be expected, the largest deviation from the desired response occurs at h=25,000 ft and M=0.4 (i.e. high and slow).

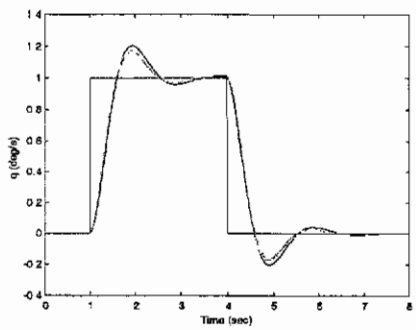

Figure 7. Linear simulations

High-fidelity, nonlinear simulations were also performed, since achieving the desired performance in linear simulations is not sufficient when assessing the controlled dynamic behavior of the highly nonlinear F-16 VISTA aircraft. The nonlinear simulations also demonstrated a predicted Level 1 pitch-rate response throughout the design envelope. Figure 8 shows the simulation results when the maneuver starts at the center of the design envelope (i.e. h=15,000 ft, M=0.6).

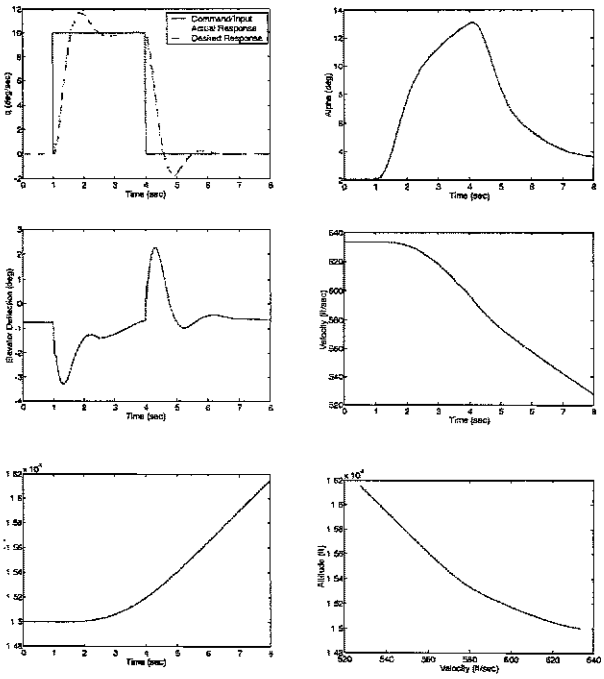

Figure 8. Nonlinear simulation

5.2 Comparison with LPV controllers

In order to assess the merits of the design procedure presented, the VISTA pitch-rate controller designed here was compared with previous LPV control designs based on μ-synthesis techniques (Spillman et al., 1996; Blue & Banda, 1997). First, comparing the results shows that the controller designed here provides better robust performance (based on μ-analysis and nonlinear simulations) than both of the LPV designs. Second, comparing the design methods revealed that the procedure presented provides a significantly more transparent design approach. Finally, comparing the architectures shows that the controller designed here is significantly easier to implement and maintain; it only requires the feedback of the pitch-rate (i.e. the controlled variable), while both LPV controllers depend on the flight condition (i.e. "automatically" gain-scheduled) and require the feedback of both the pitch-rate and the angle-of-attack. Furthermore, the controller designed here consists of just two 2^{nd} order filters, while the LPV controllers were 7^{th} and 10^{th} order systems.

6. SUMMARY

A new approach for designing large envelope controllers for high performance aircraft was presented. The procedure exploits the simplicity and transparency of both the disturbance observer control architecture and parameter-space design techniques to provide a straightforward means of designing robust large envelope flight controllers that provide explicitly defined desired closed-loop dynamics without gain-scheduling. The proeedure was demonstrated by designing a pitch-rate controller for the F-16 VISTA aircraft. The resulting controller was tested with both linear and nonlinear simulations and Level 1 handling qualities were predicted throughout the entire design envelope. Finally, the controller was compared to previous results obtained with LPV controllers that were designed with μ-synthesis techniques using the same problem formulation. Based on nonlinear simulations and μ-analysis, the controller presented here provides better robust performance, despite its significantly more simplistic architecture.

REFERENCES

J. Ackermann, A. Barlett, D. Kaesbauer, W. Sienel, and R. Steinhauser (1993). *Robust control: Systems with uncertain physical parameters*. Springer. London.

B. Aksun-Güvenç, T. Bünte, D. Odenthal, and L. Güvenç (2001). 'Robust two degree of freedom vehicle steering controller design', *Proc. of the American Control Conference*, Arlington.

P. Blue and S. Banda (1997). 'D-K iteration with optimal scales for systems with time-varying and time invariant uncertainties'. *Proc. of the American Control Conference*, Albuquerque.

T. Bünte, D. Odenthal, B. Aksun-Güvenç, and L. Güvenç (2001). 'Robust vehicle steering control based on the disturbance observer'. *Proc. of the 3rd IFAC Workshop on Advances in Automotive Control*, Karlsruhe.

L. Güvenç and K. Srinivasan (1994). 'Friction compensation and evaluation for a force control application'. *J. of Mechanical Systems and Signal Processing*, vol. 8, no. 6, pp. 623-638.

MIL-STD-1797A (1990). *Military Standard – Flying Qualities of Piloted Vehicles*

D. Odenthal and P. Blue (2000). 'Mapping of frequency response magnitude performance specifications into parameter space'. *Proc. of the 3rd IFAC Symposium on Robust Control Design*, Prague.

K. Ohnishi (1987). 'A new servo method in mechatronics'. *Trans. Japanese Soc. Elect. Eng.*, vol. 107-D, pp. 83-86.

M. Spillman, P. Blue, L. Lee, and S. Banda (1996),=. 'A robust gain scheduling example using linear parameter varying feedback', *Proc. of the 13th IFAC World Congress*, San Francisco.

T. Umeno and Y. Hori (1991), "Robust speed control of dc servomotors using modern two degrees-of-freedom controller design," *IEEE Trans. Ind. Electron.*, vol 38, no. 5, pp. 363-368.